Int. J. Heat Mass Transfer. Vol. 36, No. 7, pp. 1998–2003, 1993
Printed in Great Britain

0017–9310/93 $6.00+0.00

Transient temperature distributions within spherical products with internal heat generation and transpiration: experimental and analytical results

IBRAHIM DINCER†
Department of Refrigeration Technology, TUBITAK-Marmara Research Center, P.O. Box 21, 41470, Gebze-Kocaeli, Turkey

and

EYUP AKARYILDIZ
Department of Mechanical Engineering, Yildiz University, Yildiz-Istanbul, Turkey

(*Received* 14 *October* 1991 *and in final form* 24 *April* 1992)

INTRODUCTION

PRECOOLING is a cooling process where the field temperature of fruit and vegetables is reduced to their storage temperature in sufficient time after harvest in the field before storage or transportation [1–3]. Experimental and theoretical studies on the determination of temperature distributions, thermophysical properties, and cooling times during precooling of fruit and vegetables are at the developmental stage. Especially in the forced-air cooling of the food products, heat and mass transfer exhibit a complicated nature because of respiration heat as internal heat generation and transpiration as a result of water loss [1, 4].

A number of studies has been made in the past to relate heat and mass transfer analyses during cooling of food products [4–11]. The various methods developed for calculating heat and mass transfer in fruit and vegetables have been reviewed and discussed [8].

In order to obtain a mathematical model, we consider the fact that the convective heat transfer is more significant in the first case and is thus taken as the overall heat transfer coefficient; in the second case the overall heat transfer coefficient is the sum of the convection and radiation heat transfer coefficients; in the third case the overall heat transfer coefficient is the sum of the convection and radiation heat transfer coefficients. We also consider the effect of moisture evaporation on the convective heat transfer coefficients.

The objective of the present study is to obtain a methodology for the analysis of transient heat transfer during the cooling process, to determine the experimental and theoretical temperature distributions and the effective thermal properties of the product, and then to compare the computations with the experiments for four different air velocities.

ANALYSIS

The unique features of the mathematical model are stated in detail in ref. [1]. The assumptions made in the mathematical model are as follows:

1. Unsteady state conditions exist.
2. The rate of heat transfer in the radial direction of the spherical product is much greater than the rate in all other directions.
3. The spherical product is homogeneous and isotropic.
4. Initial temperature and water content of the product are uniform.
5. Temperature and thermal properties of the cooling medium are constant.
6. The thermal properties of the product are constant. The thermal conductivity (k) from the correlation of Sweat, thermal diffusivity (a) by the correlation of Riedel and the specific heat (C_p) from the model of Fikiin are estimated as follows [12, 13]:

$$k = 0.148 + 0.493W \tag{1}$$

$$a = 0.088 \times 10^{-6} + (a_w - 0.088 \times 10^{-6})W \tag{2}$$

$$C_p = 1.381 + 2.930W. \tag{3}$$

7. The convective and radiative heat transfer coefficients are constant. The convective heat transfer coefficient (h_c) is calculated from the following relationship for the flow of gases past single spheres [14]:

$$h_c = (k_w/D) \cdot (2.0 + 0.552 Re^{0.53} Pr^{0.33}) \quad \text{for } (1 < Re < 48\,000), \tag{4}$$

where

$$Re = U \cdot D/\nu. \tag{5}$$

The value of h_r can be calculated from the following formula [15]:

$$h_r = \sigma\varepsilon(T_s + T_a) \cdot [(T_s)^2 + (T_a)^2]. \tag{6}$$

8. The moisture rate transferred from the product during cooling is constant for different air flow velocities. The evaporation of moisture on the surface of the product subjected to forced-air cooling has an influence on the heat transfer rates, and the temperature distributions that occur within the products. Further, this produces a cooling effect at the product surfaçe due to evaporation. This effect (h_e) can be formulated as follows [16]:

$$h_e = h_c \frac{h_{fg}(W_i - W_e)}{C_p(T_i - T_e) \times 100}. \tag{7}$$

9. The rate of respiration heat affects the surface temperature. The product has a uniform heat transfer rate generated per unit mass at any point in its interior; however, this amount is a function of temperature at each point in the interior of the product.

A mathematical model in second order polynomial equation form is regressed and developed depending on the pro-

† To whom correspondence should be addressed.

NOMENCLATURE

a	thermal diffusivity [$m^2 s^{-1}$]
a_w	thermal diffusivity of water at product temperature ($=0.148 \times 10^{-6} m^2 s^{-1}$)
Bi	Biot number
C_p	specific heat [$J kg^{-1} °C^{-1}$]
D	diameter [m]
Fo	Fourier number
h	total heat transfer coefficient [$W m^{-2} K^{-1}$]
h_c	convection heat transfer coefficient [$W m^{-2} K^{-1}$]
h_e	increase in h due to evaporation [$W m^{-2} K^{-1}$]
h_{fg}	latent heat of vaporization [$J kg^{-1}$]
h_r	radiation heat transfer coefficient [$W m^{-2} K^{-1}$]
k	thermal conductivity [$W m^{-1} K^{-1}$]
p	density of product [$kg m^{-3}$]
Po	Pomerantsev number
Pr	Prandtl number
q	respiratory heat rate [$W m^{-3}$]
r	radial coordinate
R	radius [m]
Re	Reynolds number
RH	medium relative humidity [%]
t	time [s]
T	temperature [°C or K]
U	average flow velocity [$m s^{-1}$]
v	kinematic viscosity [$m^2 s^{-1}$]
W	water content [decimal].

Greek symbols

Γ	dimensionless radial distance
ε	surface emissivity (= 0.9 [8])
θ	dimensionless temperature
μ	root of transcendental equation
σ	Stefan–Boltzmann constant ($= 5.669 \times 10^{-8} W m^{-2} K^{-4}$)
ϕ	temperature difference, [°C or K].

Subscripts

a	ambient condition
c	center
e	final
exp	experimental
i	initial
n	refers to nth number
s	surface
w	water.

duct temperature using the values of respiration heat rate and temperature [1]. This model, developed for temperatures between 0 and 27°C, is given as

$$q = 0.1262618 \times 10^{-3} T^2 + 0.7061543 \times 10^{-2} T - 0.7815126 \times 10^{-2}. \quad (8)$$

We consider that the product has a uniform rate of respiratory heat generation per unit volume throughout its interior.

Consider the forced-air cooling of a spherical product of radius R, placed in an air medium of constant temperature, T_a, with a constant heat transfer coefficient, h. Three cases of h, $h = h_c$, $h = h_c + h_r$ and $h = h_c + h_r + h_e$, are investigated. At any time, the temperature distribution at all points of the spherical product is $T(R, t)$.

The differential heat transfer equation with internal heat generation in spherical coordinates can be written as

$$\frac{1}{r^2}\left[\frac{\partial}{\partial r}\left(r^2 \frac{\partial T}{\partial r}\right)\right] + \frac{q}{k} = \frac{1}{a}\frac{\partial T}{\partial t}. \quad (9)$$

The formulation of the problem in terms of the excess temperature $\phi = T - T_a$ is

$$\frac{\partial^2 \phi}{\partial r^2} + \frac{2}{r}\frac{\partial \phi}{\partial r} + \frac{q}{k} = \frac{1}{a}\frac{\partial \phi}{\partial t}. \quad (10)$$

The initial and boundary conditions are

$$\phi(r, 0) = \phi_i = T_i - T_a \quad (11)$$

$$\phi(0, t) = \text{finite} \quad (12)$$

$$-k[\partial \phi(R, t)/\partial r] = h\phi(R, t). \quad (13)$$

Consequently, the dimensionless temperature distribution at the center of the spherical product can be found as follows [17, 18]:

$$\theta_c = \frac{Po}{6}\left[1 + \frac{2}{Bi}\right] + \sum_{n=1}^{\infty}\left(1 - \frac{Po}{\mu_n^2}\right)\frac{2(Bi \sin \mu_n)}{(\mu_n - \sin \mu_n \cos \mu_n)}\exp(-\mu_n^2 Fo) \quad (14)$$

with

$$\mu_n \cot \mu_n = (1 - Bi). \quad (15)$$

Equation (15) is a transcendental equation, and the values of μ_n are roots of this equation. The Biot, Fourier, and Pomerantsev numbers are

$$Bi = hR/k \quad (16)$$

$$Fo = at/R^2 \quad (17)$$

$$Po = pqR^2/k(T_i - T_a). \quad (18)$$

The dimensionless radial distance is expressed as

$$\Gamma = r/R. \quad (19)$$

The dimensionless experimental temperature is obtained by means of experimental temperature measurements

$$\theta_{exp,c} = (T_{exp,c} - T_a)/(T_i - T_a). \quad (20)$$

EXPERIMENTAL

Apparatus

The forced-air cooling system as experimental apparatus has been designed and built in the Pilot Plant of the Refrigeration Technology Department, and used for the experimental studies. The entire experimental system consists of two main portions, which are a precooling chamber as the test section and the combined cooling unit. A schematic diagram of the experimental facility used in this study is shown in Fig. 1.

Precooling tests were carried out in the test chamber with outer dimensions of 1 × 1 × 2 m. The chamber was manufactured from 0.04 m square profiles whose surface was plated with a stainless steel sheet of 0.0005 m thickness. The inside and outside sheets were filled with glass wool to ensure heat insulation. An observation window on the door of the chamber was provided to follow the experiments. A wiper was installed to remove the condensation on the window which took place during process applications. Two separate heat exchangers that were installed on the chamber were used for providing either cooling or heating effects. In the first exchanger, 10–15°C cooling water was circulated by a pump

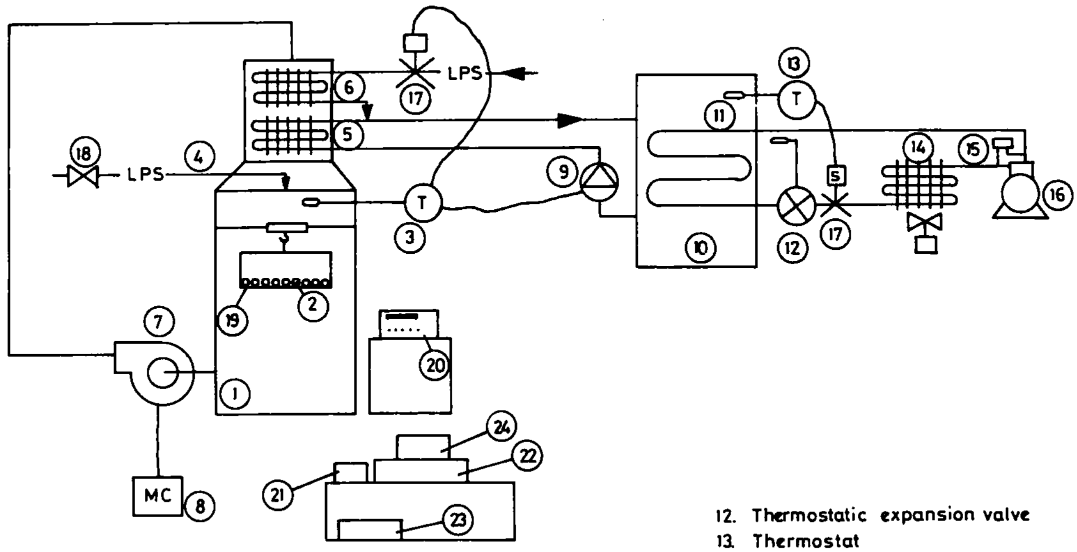

FIG. 1. Schematic diagram of the forced-air precooling system.

with power of 750 W, while 1.1–1.3 bar steam condensed in the second exchanger. A cooling effect was achieved with ethylene glycol that cooled a cooling tank of 10 tonnes capacity. In the system, a compressor of 9280 W capacity (TECUMSEH CK-99301-2 Model) was used. Two fans of 370 W capacity were used in the condensation unit. An expansion valve (R12-FLICA TMC 4.5 Model) and a RANCO combined pressostat were used for controlling the pressure.

A radial fan, having power of 1500 W and running at 2830 r.p.m., provided air flow velocities between 1.1 and 2.5 m s^{-1} in the cooling chamber. Various air velocities were achieved by the fan motor having a variable speed controller unit (SAM-EL Co. Inc., Ankara). Air was circulated through a PVC channel of 0.28 m diameter. A bellow was installed to absorb fan vibrations. The inside temperature of the chamber was controlled by a 4111 thermostat with pair contactors (ELIMKO Inc., Ankara). Two contactors were used in controlling both the solenoid valves in the cold water and steam lines. A digital temperature measurement instrument (ELIMKO Inc., Ankara) was also used to monitor the temperatures inside the chamber in the -50 to $+150$°C temperature range with Pt100 thermocouples.

The temperatures of the products and the air medium at various points were measured by a CMC 821 microprocessor device (ELLAB Instruments, Copenhagen). This device is capable of measuring to an accuracy of ± 0.1°C and has 15 channels. The response time was found to be 0.8 s. To minimize the conduction losses in these experimental investigations, the shortest temperature probes, which are DCK 8 copper–constantan thermocouples having 0.05 m length and 0.0012 m diameter, were used to measure the temperatures. The temperatures were read, displayed and printed every 30 min.

The change of relative humidity inside the test chamber was measured by a Squirrel Meter/Data Logger (Grant Instruments Ltd, Cambridge) having capacitive vaisala probes. To process the digital signals in the desired fashion, the data logger was connected to an Epson Microcomputer. The flow velocity of air over the products inside the test chamber was measured by a digital flow meter (HONTZSCH GmbH, Germany). A compression load cell connected to a digital weight indicator (α BRAN-LUEBBE Prozesse-elektronik GmbH, Germany) was used and the load was monitored. The Revere SHB-0.1-Cl model load cell and instrumentation were calibrated providing an accuracy of ± 0.001 kg at the temperature between -10 and $+40$°C.

The initial and final water contents of the products (figs) were found to be 78 and 77%, measured by drying the sample in a vacuum oven at 100°C for 24 h. Product density was determined by measuring the volume and the mass of the product.

Procedure

The experimental study was conducted to determine the temperature distributions of the spherically shaped fruits exposed to forced-air cooling at various air flow velocities. Figs of 0.047 m average diameter were used as test specimens. For each test, a sample of 5 kg from similar figs was selected and placed into a polyethylene case. The eight temperature probes were embedded at the centers of the eight products for a set of 5 kg. The other probes were used to measure the temperatures at the bottom, middle, and top of the chamber, and inlet and outlet temperatures of the cooling air. The relative humidity probes were positioned inside the chamber. After the desired temperature and relative humidity level in the chamber were reached, the case containing the products

Table 1. Test conditions and the thermophysical parameters of the product

Shape	Sphere			
D	0.047 ± 0.002 m			
p	1076 kg m^{-3}			
V	5.436×10^{-5} m^3			
T_i	22.2 ± 0.2°C			
T_e	7°C			
T_a	4 ± 0.1°C			
RH	75 ± 5%			
W_i and W_e	78 and 77%			
h_{fg}	334 000 J kg^{-1} [13]			
k	0.5325 W m^{-1} K^{-1} (equation (1))			
a	0.135×10^{-6} m^2 s^{-1} (equation (2))			
C_p	3666.4 J kg^{-1} °C^{-1} (equation (3))			
q	0.08612 W kg^{-1} (equation (8))			
Po	2.87×10^{-7} (equation (18))			
U ($m\ s^{-1}$)	Re	Case 1 $h = h_c$ ($W\ m^{-2}\ K^{-1}$)/Bi	Case 2 $h = h_c + h_r$ ($W\ m^{-2}\ K^{-1}$)/Bi	Case 3 $h = h_c + h_r + h_e$ ($W\ m^{-2}\ K^{-1}$)/Bi
1.10	3666.6	21.1/0.93	25.66/1.132	26.92/1.188
1.50	5000.0	24.7/1.09	29.26/1.291	30.73/1.356
1.75	5833.3	26.7/1.18	31.26/1.380	32.86/1.450
2.50	8333.3	32.1/1.42	36.66/1.617	38.58/1.702

was hung on the hook of the load cell and the test facility was turned on.

This procedure was repeated a total of four times for four air velocities (1.1, 1.5, 1.75 and 2.5 m s^{-1}). A detailed description of the experimental apparatus, instrumentation, procedure, data reduction techniques, and experimental results for various air velocities are given in ref. [1].

RESULTS AND DISCUSSION

In this section, the measured data are shown and compared with the predictions for three cases, namely $h = h_c$, $h = h_c + h_r$ and $h = h_c + h_r + h_e$.

The air properties used in these formulations were taken as $k = 0.0239$ W m^{-1} K^{-1}, $Pr = 0.71$, and $v = 1.41 \times 10^{-5}$ m^2 s^{-1} at a film temperature of 13.1°C, as in Holman [15]. Some experimental results of the tests performed, and theoretical results used in the model, are given in Table 1.

The respiratory heat rate (internal heat generation rate) was obtained as 0.08612 W kg^{-1} using the product initial temperature in equation (8) found by regression analysis. This heat rate for each product volume of 5.436×10^{-5} m^3 was found to be 5.037×10^{-3} W. Some simplifications could be made in equation (14) due to a negligible value of the Pomerantsev number of 2.87×10^{-7}. These are $(1 - Po/\mu_n^2) \approx 1$ and $(Po/6) \cdot (1 + 2/Bi) \approx 0$ for values of $\mu_n = 2$–11 and

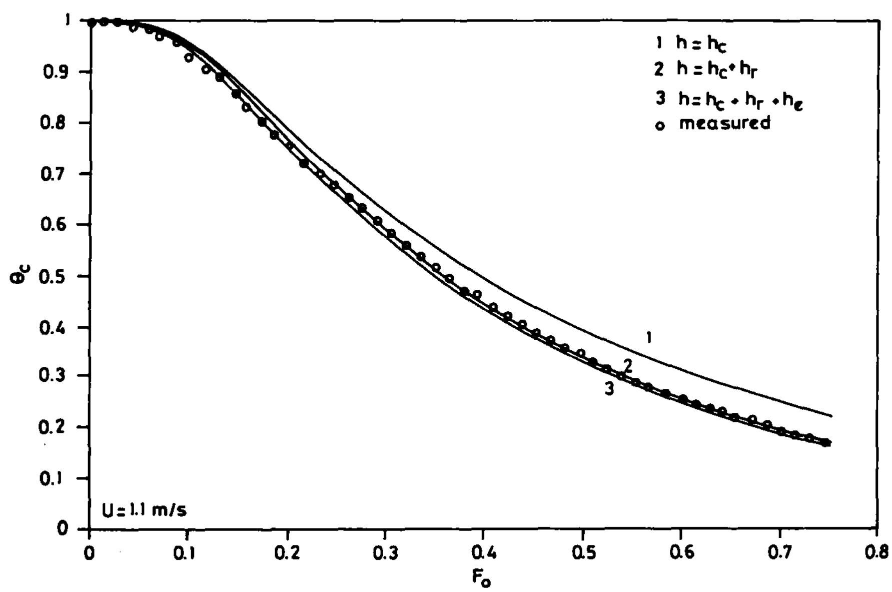

FIG. 2. Comparison of the dimensionless experimental and theoretical center temperature distributions for $U = 1.10$ m s^{-1}.

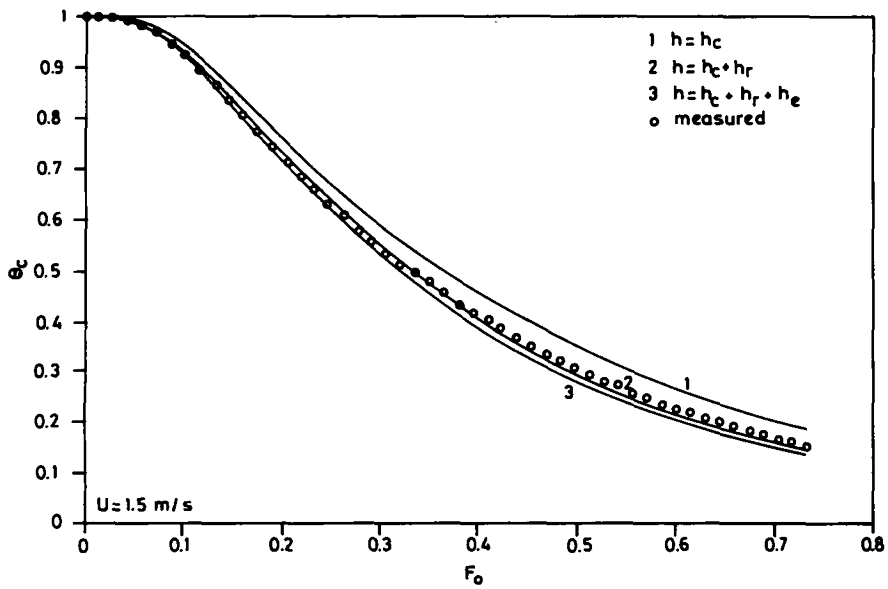

FIG. 3. Comparison of the dimensionless experimental and theoretical center temperature distributions for $U = 1.50\ \mathrm{m\ s^{-1}}$.

$Bi = 0.93$–1.702 for the three cases. Then, equation (14) can be written as

$$\theta_c = \sum_{n=1}^{\infty} \frac{(2Bi \sin\mu_n)}{(\mu_n - \sin\mu_n \cos\mu_n)} \exp(-\mu_n^2 Fo). \quad (21)$$

The complete solution is easily obtained from equation (23). In order to validate the model employed, the present results are compared with the experimental findings described earlier.

In Figs. 2–5, the experimental and theoretical results for three cases at different air velocities are presented, and a representative set of such comparisons is shown. These figures are typical Fourier number–dimensionless temperature profiles showing the experimental and predicted product center temperature distributions. It is clear from Figs. 2–5 that all the measured and computed profiles decrease monotonically with increasing Fourier number. The results obtained indicate that the cooling rate of the product increases with increasing air velocity. At this point, a higher cooling rate is provided at a higher air velocity.

As illustrated in Figs. 2–5 for four air velocities (1.1, 1.5, 1.75 and 2.5 $\mathrm{m\ s^{-1}}$), the maximum error between the measured and analytical results is found to be around $\pm 20\%$ for the first case ($h = h_c$). However, a large majority of the results are within $\pm 8\%$ for the second case ($h = h_c + h_r$), and within

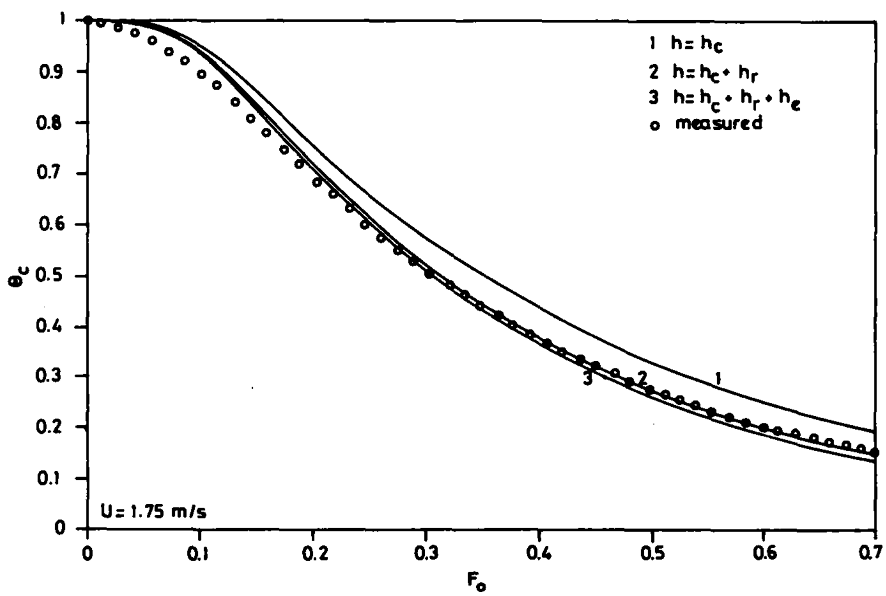

FIG. 4. Comparison of the dimensionless experimental and theoretical center temperature distributions for $U = 1.75\ \mathrm{m\ s^{-1}}$.

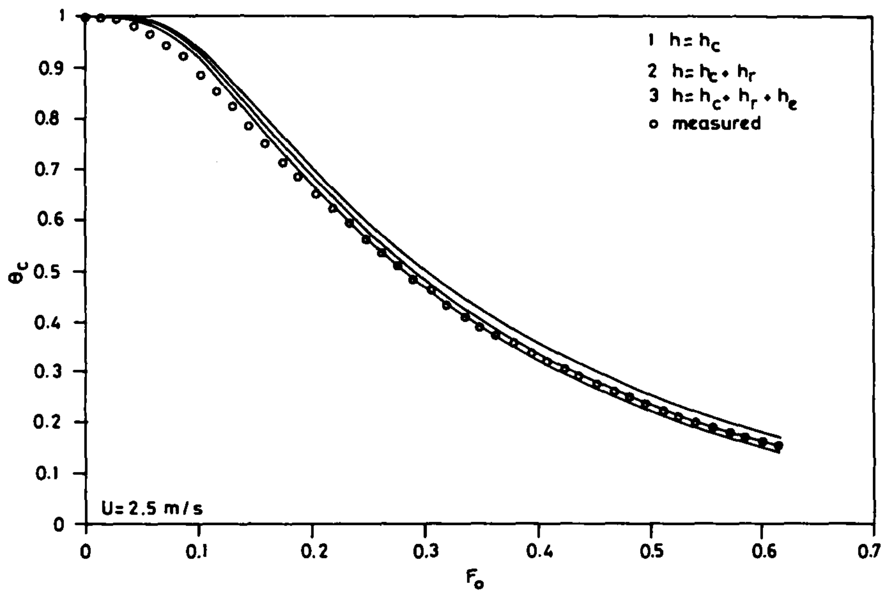

FIG. 5. Comparison of the dimensionless experimental and theoretical center temperature distributions for $U = 2.50\ \mathrm{m\ s^{-1}}$.

$\pm 5\%$ for the third case ($h = h_c + h_r + h_e$). This shows that the third case is the most realistic case and this remarkably good agreement between the measured and computed results for the third case indicates that the approach developed is a feasible and accurate method for the solution of this type of problem.

In order to minimize the system transients due to temperature measurements, an average value from eight readings was used for all cases.

REFERENCES

1. I. Dincer, Experimental and theoretical heat and mass transfer studies on the forced-air precooling of spherical food products, M.Sc. Thesis, Mech. Engng Dept., Yildiz University, Istanbul (1991).
2. I. Dincer, Estimation of the temperature distributions in the hydrocooling of spherical products, *4th Int. Symp. on Transport Phenomena in Heat and Mass Transfer*, Sydney (14–18 July 1991).
3. I. Dincer, A simple model for estimation of the film coefficients during cooling of certain spherical foodstuffs with water. *Int. Commun. Heat Mass Transfer* **18,** 431–443 (1991).
4. F. A. Ansari, V. Charan and H. K. Varma, Heat and mass transfer analysis in air-cooling of spherical food products, *Int. J. Refrigeration* **7,** 194–197 (1984).
5. F. A. Ansari and A. Afaq, Precooling of the cylindrical food products, *Int. J. Refrigeration* **9,** 161–163 (1986).
6. C. D. Baird and J. J. Gaffney, A numerical procedure for calculating heat transfer in bulk loads of fruits and vegetables, *ASHRAE Trans.* **82,** 525–535 (1976).
7. J. J. Gaffney, C. D. Baird and K. V. Chau, Influence of airflow rate, respiration, evaporative cooling, and other factors affecting weight loss calculations for fruits and vegetables, *ASHRAE Trans.* **91,** 690–707 (1985).
8. J. J. Gaffney, C. D. Baird and K. V. Chau, Methods for calculating heat and mass transfer in fruits and vegetables individually and in bulk, *ASHRAE Trans.* **91,** 333–352 (1985).
9. D. R. Guemes, M. E. Pirovani and J. H. di Pentima, Heat transfer characteristics during air precooling of strawberries, *Int. J. Refrigeration* **12,** 169–173 (1988).
10. K. Hayakawa and J. Succar, Heat transfer and moisture loss of spherical fresh produce, *J. Food Sci.* **47,** 595–605 (1982).
11. S. K. Sastry, C. A. Zuritz and A. Anantheswaran, Interaction between heat and mass transfer in foods, *ASHRAE Trans.* **91,** 353–370 (1985).
12. V. E. Sweat, Thermal properties of foods. In *Engineering Properties of Foods* (Edited by M. A. Rao and S. S. H. Rizvi), pp. 49–87. Marcel Dekker, New York (1986).
13. *ASHRAE Handbook of Fundamentals.* American Society of Heating, Refrigerating and Air-Conditioning Engineers, Atlanta, GA (1981).
14. C. J. Geankoplis, *Transport Processes and Unit Operations.* Allyn & Bacon, Boston, MA (1978).
15. J. P. Holman, *Heat Transfer.* McGraw-Hill, New York (1976).
16. S. R. Suntur, *Besinleri Sogukta Saklama Teknolojisi.* Caglayan Yayinevi, Istanbul (1982).
17. V. S. Arpaci, *Conduction Heat Transfer.* Addison-Wesley, Reading, MA (1966).
18. A. V. Luikov, *Analytical Heat Diffusion Theory.* Academic Press, New York (1968).